Frustrated trimer chain model and $Cu_3Cl_6(H_2O)_2{\cdot}2H_8C_4SO_2$ in a magnetic field

A. Honecker[1] and A. Läuchli[2]
[1] *Institut für Theoretische Physik, TU Braunschweig, Mendelssohnstr. 3, D–38106 Braunschweig, Germany.*
[2] *Institut für Theoretische Physik, ETH-Hönggerberg, CH–8093 Zürich, Switzerland.*
(May 24, 2000; revised October 13, 2000)

Recent magnetization and susceptibility measurements on $Cu_3Cl_6(H_2O)_2{\cdot}2H_8C_4SO_2$ by Ishii *et.al.* [J. Phys. Soc. Jpn. **69**, 340 (2000)] have demonstrated the existence of a spin gap. In order to explain the opening of a spin gap in this copper-trimer system, Ishii *et.al.* have proposed a frustrated trimer chain model. Since the exchange constants for this model have not yet been determined, we develop a twelfth-order high-temperature series for the magnetic susceptibility and fit it to the experimentally measured one. We find that some of the coupling constants are likely to be *ferromagnetic*. The combination of several arguments does not provide any evidence for a spin gap in the parameter region with ferromagnetic coupling constants, but further results e.g. for the magnetization process are in qualitative agreement with the experimental observations.

PACS numbers: 75.50.Ee, 75.40.Mg, 75.45.+j

I. INTRODUCTION

The trimerized $S = 1/2$ Heisenberg chain in a strong external magnetic field has already received a substantial amount of theoretical attention, one reason being a plateau at one third of the saturation magnetization in the magnetization curve [1–5]. Some frustrated variants of the trimer model have also been investigated [6–10] since they can be shown to have dimer groundstates and thus a spin gap.

While many materials with trimer constituents exist (see e.g. [11]), the behavior in high magnetic fields has been investigated only in a few of them, for instance in $3CuCl_2{\cdot}2$dioxane [12]. Also $Cu_3Cl_6(H_2O)_2{\cdot}2H_8C_4SO_2$ belongs to the known trimer materials [13,14], but its behavior in a strong magnetic field has been measured only recently [15] and at the same time its magnetic susceptibility has been remeasured. Surprisingly, a spin gap of about 3.9Tesla (that is roughly 5.5K) is observed both in the magnetic susceptibility of $Cu_3Cl_6(H_2O)_2{\cdot}2H_8C_4SO_2$ [16] as well as in the magnetization as a function of external magnetic field. This system probably exhibits also a plateau at one third of the saturation magnetization in addition to the spin gap.

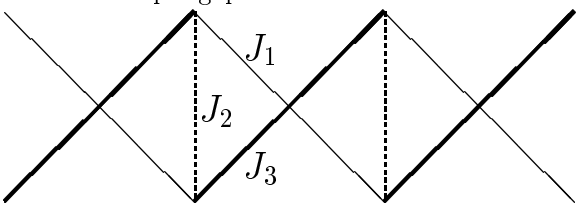

FIG. 1. The frustrated trimer chain model. All corners and intersections carry a spin 1/2 coupled with exchange constants indicated by the connecting lines.

Motivated by the crystal structure [13], the authors of [15] have proposed the following model (see also Fig. 1) [17]:

$$\begin{aligned} H = {} & J_1 \sum_{i=1}^{L/3} \{\mathbf{S}_{3i} \cdot \mathbf{S}_{3i+1} + \mathbf{S}_{3i+1} \cdot \mathbf{S}_{3i+2}\} \\ & + J_2 \sum_{i=1}^{L/3} \mathbf{S}_{3i+2} \cdot \mathbf{S}_{3i+3} \\ & + J_3 \sum_{i=1}^{L/3} \{\mathbf{S}_{3i+1} \cdot \mathbf{S}_{3i+3} + \mathbf{S}_{3i+2} \cdot \mathbf{S}_{3i+4}\} \\ & - h \sum_{i=1}^{L} S_i^z \,. \end{aligned} \tag{1.1}$$

Since the spin is localized on Cu^{2+} ions, the $\mathbf{S}_i$ are spin-1/2 operators at site i. In (1.1), the reduced field h is related to the physical field H by $h = g\mu_B H$ in units where $k_B = 1$. The numerical prefactor is determined by $\mu_B \approx 0.67171\mathrm{K/Tesla}$ as well as the value of g which for the present material is slightly above 2 (the precise numerical value depends on the direction of the external magnetic field relative to the crystal axes).

For a study of the phase diagram of the Hamiltonian (1.1), it is useful to observe that the Hamiltonian and therefore also the phase diagram are invariant under the exchange of J_1 and J_3 such that one can concentrate e.g. on $|J_3| \leq |J_1|$. In fact, the $h = 0$ phase diagram with antiferromagnetic exchange constants ($J_i \geq 0$) has been explored in [18] using bosonization and exact diagonalization (see also [19]) determining in particular a parameter region with a spin gap. Very recently, this was complemented by a computation of the magnetization curve at some values of the parameters using DMRG [20]. The investigations of [18–20] concentrated on the region with all coupling constants in (1.1) antiferromagnetic ($J_i \geq 0$) because [15] suggested that this should be appropriate for $Cu_3Cl_6(H_2O)_2{\cdot}2H_8C_4SO_2$. However, the parameters

relevant to the experimental system have not really been determined so far. We believe that this is an important issue in particular in view of the fact that according to the crystallographic data [13], all angles of the Cu–Cl–Cu bonds lie in the region of 91° to 96° – a region where usually no safe inference on the coupling constants J_i can be made, not even about their signs. We will therefore develop a high-temperature series for the magnetic susceptibility of the model (1.1) and use it to *determine* the coupling constants from the experimental data [15]. It will turn out that some coupling constants are likely to be *ferromagnetic*, *i.e.* the experimentally relevant coupling constants lie presumably outside the region studied so far. We then proceed to study more general properties of the model and to address the question of a spin gap in the relevant parameter region. We use mainly perturbative arguments supplemented by numerical methods.

Some supplementary results on the trimer model are contained in the appendices or can be found in [21].

II. MAGNETIC SUSCEPTIBILITY AND SPECIFIC HEAT

A. High-temperature series for zero field

First we discuss some high-temperature series in zero magnetic field. We have used an elementary approach to perform the computations. Denote the Hamiltonian of a length L chain with $h = 0$ by H_0. Then the fundamental ingredient for any higher-order expansion is that contributions of $\mathrm{tr}\left(H_0^N\right)$ to suitable physical quantities become independent of the system size L if one uses a long enough chain with periodic boundary conditions. The concrete Hamiltonian H_0 given by (1.1) must be applied $2L/3$ times to wind once around the system and to feel that it is finite. On the other hand, contributions from $\mathrm{tr}\left(H_0^N\right)$ with $N < 2L/3$ are independent of L. We have used this observation to determine the high-temperature series by simply computing the traces for the lowest powers N on a chain with a fixed L and periodic boundary conditions [22]. Just two small refinements to this elementary approach have been made. The first one is that we computed the traces separately for all subspaces of the z-component of the total spin S^z_{tot}. This is already sufficient to obtain series for the specific heat c_v and the magnetic susceptibility χ. The second one is to make also the order $2L/3$ usable: At this order, only the coefficient of $J_1^{L/3} J_3^{L/3}$ is affected by the finiteness of the chain and this coefficient can be corrected by hand using results for a Heisenberg ring of length $2L/3$.

For notational convenience, we introduce the partition function for L sites by

$$Z_L = \mathrm{tr}\left(\mathrm{e}^{-\beta H_0}\right) \tag{2.1}$$

with $k_B T = 1/\beta$.

The lowest orders of a reduced magnetic susceptibility χ are found to be

$$\begin{aligned}
\chi_{\mathrm{red.}}(\beta) &= \frac{1}{\beta L Z_L} \frac{\partial^2}{\partial h^2} \mathrm{tr}\left(\mathrm{e}^{-\beta\left(H_0 - h S^z_{\mathrm{tot}}\right)}\right)\Big|_{h=0} = \frac{\beta}{L} \frac{\mathrm{tr}\left(\left(S^z_{\mathrm{tot}}\right)^2 \mathrm{e}^{-\beta H_0}\right)}{Z_L} \\
&= \frac{\beta}{4} - \frac{\beta^2}{24}\left(2J_3 + J_2 + 2J_1\right) - \frac{\beta^3}{96}\left(J_1^2 + J_2^2 + J_3^2 - 6J_3J_1 - 2J_2J_1 - 2J_3J_2\right) \\
&\quad + \frac{\beta^4}{1152}\left(8J_3^3 - 3J_3^2J_2 + 6J_2^2J_1 + 6J_3J_2^2 + 8J_1^3 - 3J_2J_1^2 + J_2^3\right) \\
&\quad + \frac{\beta^5}{4608}\left(-28J_3^2J_2J_1 - 28J_3J_1^2J_2 + 36J_3^2J_1^2 + 8J_3^2J_2^2 + 8J_2^2J_1^2 - 2J_2^3J_1 - 34J_3J_1^3 - 34J_3^3J_1\right. \\
&\qquad \left. - 10J_2J_1^3 - 2J_3J_2^3 - 10J_3^3J_2 - 28J_3J_1J_2^2 + 14J_1^4 + 14J_3^4 + 5J_2^4\right) \\
&\quad + \mathcal{O}\left(\beta^6\right) .
\end{aligned} \tag{2.2}$$

Similarly, we obtain the lowest orders of the high-temperature series for the specific heat

$$\begin{aligned}
\frac{c_v(\beta)}{k_B} &= \frac{\beta^2}{L} \frac{\partial^2}{\partial \beta^2} \ln\left(Z_L\right) \\
&= \frac{\beta^2}{16}\left(2J_1^2 + J_2^2 + 2J_3^2\right) + \frac{\beta^3}{32}\left(2J_3^3 + 2J_1^3 + J_2^3 - 6J_3J_1J_2\right) \\
&\quad - \frac{\beta^4}{256}\left(8J_3^2J_2J_1 + 8J_3J_1^2J_2 + 12J_3^2J_1^2 + 8J_3^2J_2^2 + 8J_2^2J_1^2 + 6J_1^4 + 6J_3^4 + J_2^4 + 8J_3J_1J_2^2\right) \\
&\quad + \mathcal{O}\left(\beta^5\right) .
\end{aligned} \tag{2.3}$$

Complete 12th order versions of both series can be accessed via [21].

For a uniform Heisenberg chain ($J_1 = J_2$ and $J_3 = 0$), the coefficients of the series for χ and $\ln\left(Z_L\right)/L$ (or c_v) agree with those given for instance in [23] when they overlap.

B. Fit to the experimental susceptibility

Now we use our 12th order series for the susceptibility (2.2) to fit the experimental data [15] and thus extract values for the coupling constants J_i. We used the data for the single crystal ($H \parallel b$-axis) and the polycrystalline sample [15] as well as some unpublished new measurements for all three axes of a single crystal [24]. For the polycrystalline case the average g-factor is known to be $g_{\rm av} \approx 2.1$ from ESR while in the single crystal case [15] we used the g-factor as a fitting parameter. The following prefactors are used to match the series (2.2) to the experimental data:

$$\chi_{\rm exp.}(T) = \frac{3N_A g^2 \mu_B^2}{k_B}\, \chi_{\rm red.}\left(\frac{1}{T}\right) . \qquad (2.4)$$

We performed fits in various intervals of temperature with a lower boundary (T_l) lying between 150K and 250K, while the upper boundary was kept fixed at 300K. Fits were performed with the raw 12th order series. For both experimental data sets of [15] we obtained reasonable, though volatile fits around $T_l = 150\text{K} - 250\text{K}$ yielding the following estimates: $J_1 = -250\text{K} \pm 40\text{K}$, $J_2 = 250\text{K} \pm 40\text{K}$, $J_3 = -40\text{K} \pm 30\text{K}$. For the single crystal sample we additionally determined $g_b = 1.95 \pm 0.05$.

We have further performed fits to unpublished single-crystal data sets where the g-factors are known from ESR [24]. When a constant is added to (2.2), the data for all three crystal axes can be fitted consistently with $J_1 \approx -300\text{K}$, $J_2 \approx 280\text{K}$ and $J_3 \approx -60\text{K}$ in an interval of high temperatures ($220\text{K} \lesssim T \leq 300\text{K}$). This set of coupling constants is in agreement with our earlier fits and we will use the latter in the further discussion below.

Fig. 2 shows the measured susceptibility for the polycrystalline sample [15] together with the series result. Since the parameters were obtained from a fit which was performed with a different data set, we have used $g = 2.03$ (which differs slightly from the experimentally found $g_{\rm av} \approx 2.1$) in order to obtain agreement of the raw series with the experimental data for $T \geq 240\text{K}$. Clearly, the raw series should not be trusted down into the region of the maximum of χ where Padé approximants should be used instead. The region below the maximum cannot be expected to be described with a high-temperature series. The overall agreement is reasonable though the theoretical result reproduces the experimental one in the vicinity of the maximum only qualitatively. This discrepancy might be due to the frustration in the model which leads to cancellations in the coefficients. Note also that, due to the frustration, the maximum of χ is located at a lower temperature than would be expected for a non-frustrated model with coupling constants of the same order of magnitude. Consequently, higher orders are important in the entire temperature range covered by Fig. 2, precluding in particular the analysis of the high-temperature tail of χ in terms of a simple Curie-Weiss law.

The agreement for intermediate temperatures can be improved if the maximum is included in the fitting region and Padé approximants are used in the fit. The main change with respect to the fits discussed above is that J_3 tends to be closer to J_1. However, it will become clear from the discussion in later sections that the region with J_3 close to J_1 is not appropriate to describe the experimental observations of the low-temperature region.

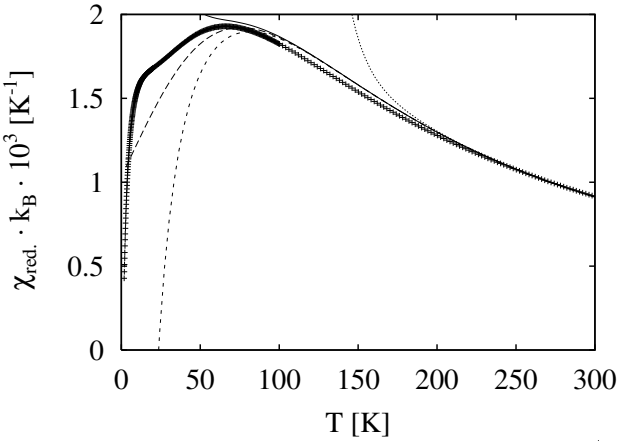

FIG. 2. Experimental results for the susceptibility ('+') in comparison with the fit $J_1 = -300\text{K}$, $J_2 = 280\text{K}$ and $J_3 = -60\text{K}$. We show the raw 12th order series (dotted line) as well as several Padé approximants: [7,6] (full line), [6,6] (long dashes) and [6,5] (short dashes).

Although we are not able to determine the coupling constants to high accuracy, all our fits lead to the conclusion that J_2 should be antiferromagnetic and J_1 and J_3 (or at least one of them) must be *ferromagnetic* if one wants to model the susceptibility measured at high temperatures [15] with the frustrated trimer chain (1.1). In view of earlier theoretical investigations [18–20], this conclusion is somewhat surprising. Note that none of our fits converged to all $J_i > 0$. Additional assumptions (including a constraint on the J_i) are necessary to determine from $\chi(T)$ what the optimal values of the J_i would be in this antiferromagnetic region and thus allow for a comparison with Fig. 2. Such a fit and a comparison with the present one is discussed in appendix A. The upshot is that the experimentally observed $\chi(T)$ [15] cannot be explained with only antiferromagnetic J_i.

The findings of this section necessitate a detailed reanalysis of the Hamiltonian (1.1) since earlier works did not look at the appropriate parameter region.

III. LANCZOS RESULTS

In order to study the zero-temperature behavior of the frustrated trimer chain we have performed Lanczos diagonalizations of small clusters with periodic boundary conditions. Although computations were performed for various values of the parameters, we will present explicit results only for the final parameter set determined above.

Further results in the region $J_i > 0$ are in agreement with [18–20] and are used in appendix A.

Fig. 3 presents the zero-temperature magnetization curve for the trimer chain model. Here and below the magnetization $\langle M \rangle$ is normalized to saturation values ± 1. First, it is reassuring that the system still has antiferromagnetic features despite two ferromagnetic coupling constants (note that we are now probing a region far from that used for determining the J_i). Since experiments found a spin gap [15], an important question clearly is if we also obtain a gap from the model with these parameters. We have therefore performed a finite-size analysis of the gap to $S^z = 1$ excitations (corresponding to the first step in the finite-size magnetization curves of Fig. 3). All our approaches led to results compatible with a vanishing gap. However, it is difficult to reliably exclude a gap of a few K with system sizes $L \leq 30$. We will therefore return to this issue later and assume for the extrapolated thick line in Fig. 3 a vanishing spin gap. In general, this extrapolation was obtained by connecting the mid-points of the steps of the $L = 30$ magnetization curve, except for $\langle M \rangle = 1$ and $\langle M \rangle = 1/3$ where the corners were used.

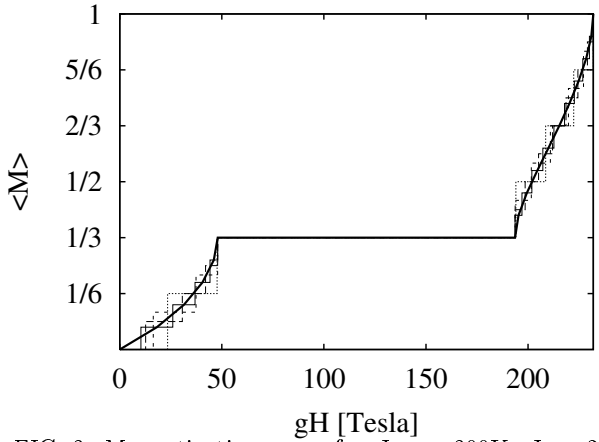

FIG. 3. Magnetization curve for $J_1 = -300$K, $J_2 = 280$K and $J_3 = -60$K. The thick line is an extrapolation whereas thin lines are for finite system sizes: $L = 12$ (dotted), $L = 18$ (short dashes), $L = 24$ (long dashes) and $L = 30$ (full).

For the parameters of Fig. 3, $\langle M \rangle = 1/3$ is reached with a magnetic field $H = 20 - 25$Tesla. The order of magnitude agrees with the experimental finding [15] even if the value found within the model is a factor of two to three below the experimental one. Above this field, Fig. 3 exhibits a clear $\langle M \rangle = 1/3$ plateau which is expected on general grounds [1–5].

We conclude this section by presenting in Fig. 4 the lowest three excitations for the $S^z = 1$ sector as a function of momentum k, where k is measured with respect to the groundstate, *i.e.* $k = k_{S^z=1} - k_{\rm GS}$. This spectrum is very similar to that of an $S = 1/2$ Heisenberg chain of length $L/3$ with coupling constant $J_{\rm eff.} \approx 16$K. In particular, one can recognize the two-spinon scattering continuum and a few higher excitations. This identification of the low-energy excitations of the frustrated trimer chain with an effective $S = 1/2$ Heisenberg chain is one of the numerical indications for the absence of a spin gap.

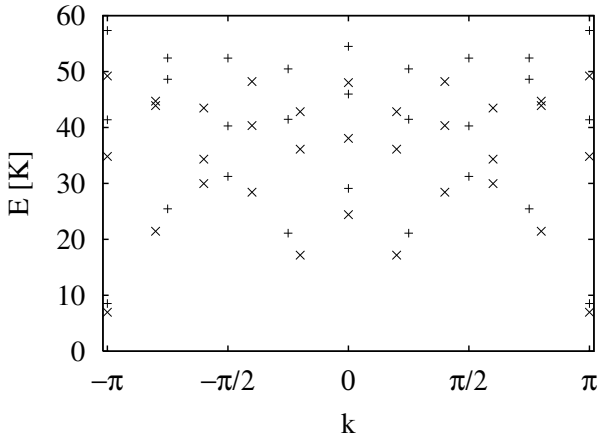

FIG. 4. Lowest three excitations in the $S^z = 1$ sector for $L = 24$ ('+') and $L = 30$ ('×') with $J_1 = -300$K, $J_2 = 280$K and $J_3 = -60$K.

IV. THE LINE $J_1 = J_3$

The Lanczos results of the previous section raise the question if the trimer chain model has a spin gap in the region with J_1, $J_3 < 0$: In this region, the model behaves like an antiferromagnet (see e.g. Fig. 3) which is frustrated since the number of antiferromagnetic coupling constants around a triangle is odd. Therefore, a spin gap appears possible in principle and we proceed with further arguments to decide whether it appears in the relevant parameter region.

Evidence for a spin gap in the parameter region J_1, $J_3 > 0$ was actually first obtained on the line $J_1 = J_3$ [10]. The reason is presumably that the line $J_1 = J_3$ can be treated analytically at least to some extent because then the total spin is locally conserved on each bond coupled by J_2. In fact, one can easily discuss the entire magnetization process [25] and not just the question of a spin gap and we refer the interested reader to [21] for some comments on this aspect.

Recall that the model (1.1) with $h = 0$ gives rise to three types of groundstates in different regions with $J_1 = J_3 > 0$ (we will assume $J_2 > 0$ throughout this section) [10]: That of the $S = 1/2$-$S = 1$ ferrimagnetic chain for $J_2 < 0.90816 J_1$, a spontaneously dimerized state for $0.90816 J_1 < J_2 < 2J_1$ and, finally, singlets are formed on all bonds coupled by J_2 for $J_2 > 2J_1$ with effectively free spins in between. In the first and the third case, one finds ferrimagnetic behavior with a spontaneous magnetization $\langle M \rangle = 1/3$ and only the second region exhibits the requested gap.

For $J_1 = J_3 < 0$, we found only two regions:

1. For

$$J_2 > -J_1 \tag{4.1}$$

the groundstate is formed by singlets on the J_2-bonds and free $S = 1/2$ spins in between. This again gives rise to ferrimagnetic behavior with a spontaneous magnetization $\langle M \rangle = 1/3$.

2. When

$$J_2 < -J_1 \tag{4.2}$$

the entire system behaves like a ferromagnet. In this case the system is spontaneously completely polarized ($\langle M \rangle = 1$).

We conclude that –unlike for $J_1 = J_3 > 0$– the groundstate is always gapless for $J_1 = J_3 < 0$ which we have argued to be more appropriate for $Cu_3Cl_6(H_2O)_2{\cdot}2H_8C_4SO_2$.

V. EFFECTIVE HAMILTONIANS FOR THE GROUNDSTATE

The low-energy behavior of the model Hamiltonian (1.1) can be analyzed further using degenerate perturbation theory. Truncation at a certain order of the coupling constants leads to effective Hamiltonians which in some cases turn out to be well-known models.

We will use the abbreviations

$$\tilde{J}_i = \frac{J_i}{J_1}, \qquad \bar{J}_i = \frac{J_i}{J_2}. \tag{5.1}$$

A. J_1 large and antiferromagnetic

To test the method, we first consider the case of antiferromagnetic J_1. For this purpose we extend the first-order effective Hamiltonian of [20] for the case $J_1 \gg J_2$, $J_3 \geq 0$ to second order. For J_1 large and antiferromagnetic, the groundstate-space of a trimer is given by an $S = 1/2$ representation. In this subspace of doublets, the effective Hamiltonian has the form of a J_1-J_2 chain when truncated after the second order:

$$H_{\text{eff.}} = \mathcal{J}_1 \sum_i \mathbf{S}_i \cdot \mathbf{S}_{i+1} + \mathcal{J}_2 \sum_i \mathbf{S}_i \cdot \mathbf{S}_{i+2}. \tag{5.2}$$

Here, the $\mathbf{S}_i$ are effective spin-1/2 operators. The effective exchange constants are

$$\frac{\mathcal{J}_1}{J_1} = \frac{4}{9}\left(-\tilde{J}_3 + \tilde{J}_2\right) - \frac{79}{405}\tilde{J}_3^2 + \frac{8}{135}\tilde{J}_2\tilde{J}_3 + \frac{211}{1620}\tilde{J}_2^2 \tag{5.3}$$

and

$$\frac{\mathcal{J}_2}{J_1} = -\frac{91}{486}\tilde{J}_3^2 + \frac{22}{243}\tilde{J}_2\tilde{J}_3 + \frac{10}{243}\tilde{J}_2^2. \tag{5.4}$$

In this approximation, the ferrimagnetic phase found in [18] is given by an effective ferromagnetic Hamiltonian ($\mathcal{J}_1 < 0$) while the antiferromagnetic phase corresponds to $\mathcal{J}_1 > 0$. The transition line can thus be determined from $\mathcal{J}_1 = 0$ [26]. We find

$$\begin{aligned}\tilde{J}_3 &= \frac{12}{79}\tilde{J}_2 - \frac{90}{79} + \frac{1}{158}\sqrt{17245\tilde{J}_2^2 + 48240\tilde{J}_2 + 32400} \\ &= \tilde{J}_2 - \frac{1}{80}\tilde{J}_2^2 + \mathcal{O}\left(\tilde{J}_2^3\right),\end{aligned} \tag{5.5}$$

which improves the agreement of the approximation $\tilde{J}_3 = \tilde{J}_2$ [20] with the numerical results of [18].

The dimer phase with a spin gap is characterized by $\mathcal{J}_2/\mathcal{J}_1 > 0.241167(5)$ (see [27] and references therein). Using (5.3) and (5.4), it is found to open at $\tilde{J}_2 \approx 3.60$, $\tilde{J}_3 \approx 1.361$ with a square-root like behavior of $\tilde{J}_3$ as a function of $\tilde{J}_2$. Since this is not in the weak-coupling region, it is not surprising that the numbers differ substantially from those obtained numerically in [18]. However, the topology of the groundstate phase diagram comes out correctly from our effective Hamiltonian: In particular, the dimerized spin gap phase is located inside the antiferromagnetic phase and arises because of a sufficiently large effective second neighbor frustration $\mathcal{J}_2$.

B. J_2 large and antiferromagnetic

The preceding argumentation is not applicable to the region $J_2 > 0$, $J_1, J_3 < 0$. However, a similar case has been discussed earlier [1,4] and $J_2 \gg |J_1|, |J_3|$ has been found to be a useful limiting case. We will now analyse this region in the same manner as above.

For $J_2 \gg |J_1|, |J_3|$, the spins on all J_2-bonds couple to singlets and only the intermediate spins contribute to the low-energy excitations. In the space of these intermediate spins, we can again map the Hamiltonian (1.1) to the Hamiltonian (5.2) to the lowest orders in J_1, J_3. Up to fifth order, we find the effective coupling constants to be given by [28]

$$\begin{aligned}\frac{\mathcal{J}_1}{J_2} = \left(\bar{J}_1 - \bar{J}_3\right)^2 \Bigg\{ &\frac{1}{2} + \frac{3\left(\bar{J}_1 + \bar{J}_3\right)}{4} + 3\bar{J}_1\bar{J}_3 \\ &- \frac{\left(\bar{J}_1 + \bar{J}_3\right)\left(107\left(\bar{J}_1^2 + \bar{J}_3^2\right) - 406\bar{J}_1\bar{J}_3\right)}{64} \Bigg\}\end{aligned} \tag{5.6}$$

and

$$\frac{\mathcal{J}_2}{J_2} = \frac{\left(\bar{J}_1 + \bar{J}_3\right)\left(\bar{J}_1 - \bar{J}_3\right)^4}{4}. \tag{5.7}$$

This mapping is now applicable regardless of the sign of J_1 and J_3 as long as $J_2 > 0$. First we consider the case of antiferromagnetic $J_1, J_3 > 0$. Then the effective coupling constants are essentially always antiferromagnetic, *i.e.* $\mathcal{J}_1, \mathcal{J}_2 > 0$ leading to a frustrated chain. If J_1 and

J_3 are large enough, $\mathcal{J}_2/\mathcal{J}_1$ can exceed the critical value of about 0.241 (see above) and a spin gap opens. These observations are again in qualitative agreement with the phase diagram of [18]. As for the preceding limit, one should not expect good quantitative agreement since the required values of J_1 and J_3 are not small but of the same order as J_2.

Now we turn to the more interesting case $J_1, J_3 < 0$. Then the oupling constant (5.7) is always ferromagnetic: $\mathcal{J}_2 < 0$. If $|J_1|$ and $|J_3|$ are large enough, $\mathcal{J}_1$ also becomes ferromagnetic. This is compatible with the behavior found in section IV on the line $J_1 = J_3 < 0$. If $|J_1|$ and $|J_3|$ are small, $\mathcal{J}_1$ remains antiferromagnetic. Since $\mathcal{J}_2$ is always ferromagnetic, no frustration arises in the effective model and a spin gap is *not* expected to open. This is true to the order which we have considered. Higher orders might actually yield frustrating contributions. In any case, frustration is substantially weaker for ferromagnetic $J_1, J_3 < 0$ than for antiferromagnetic $J_1, J_3 > 0$. It is therefore plausible that a spin gap is absent in the ferromagnetic region (unless $|J_1|$ and/or $|J_3|$ are very large and the present argument is not applicable).

It should be noted that (5.6) and (5.7) turn out to be small if $\bar{J}_1 - \bar{J}_3$ is small. In fact, one can argue that the results of this section remain qualitatively correct for $\bar{J}_1 - \bar{J}_3$ small even if $\bar{J}_1$ and $\bar{J}_3$ are not separately small: For $J_1 = J_3$, the intermediate spins are effectively decoupled due to the presence of the singlets on the J_2-bonds (see section IV). A small detuning $J_1 \neq J_3$ generates an effective coupling of the intermediate spins via higher-order processes. However, the effective coupling will stay small as long as $J_1 - J_3$ is small. If one wants to model $Cu_3Cl_6(H_2O)_2{\cdot}2H_8C_4SO_2$, $|J_1 - J_3|$ must therefore at least be on the same scale as e.g. the field $h \approx 80$K required to polarize the intermediate spins leading to $\langle M \rangle = 1/3$ [15]. This observation rules out a J_1 very close to J_3.

Finally, we also calculated the effective Hamiltonian for a strong ferromagnetic intra-trimer interaction J_1. The problem then maps to a frustrated $S = 3/2$ chain with four-spin interactions. Even if this is not a well-known Hamiltonian and the issue of a spin gap thus remains unclear in this case, we present it in appendix B in order to open the way for further investigation of this limit.

VI. MAGNETIZATION PLATEAUX

We complete our theoretical analysis with a discussion of plateaux in the magnetization curves of the frustrated trimer chain model.

A plateau with $\langle M \rangle = 1/3$ is abundant in the magnetization curve (compare Fig. 3) and can be easily understood in the limits $|J_2|, |J_3| \ll J_1$ or $|J_1|, |J_3| \ll J_2$. This is readily done by adding the coupling J_3 to the series of [4]. More details as well as the explicit series for the boundaries of the $\langle M \rangle = 1/3$ plateau are available under [21]. Here we just mention that the main conclusions of [4] regarding this plateau remain qualitatively unchanged in the presence of the additional coupling J_3.

Regarding plateaux with $\langle M \rangle \neq 1/3$, observe first that, when a spin gap opens in the frustrated trimer model, the groundstate is dimerized, *i.e.* translational invariance is spontaneously broken by a period two. Spontaneous breaking of translational invariance by a period two also permits the appearance of a plateau with $\langle M \rangle = 2/3$ (see [29] and references therein). We will now investigate this possibility further.

First we consider the case $J_1 > 0$ and start in the limit of strong trimerization ($J_2 = 0, J_3 = 0$). When one applies a magnetic field $h_c = \frac{3}{2}J_1$, the two states $|{\uparrow\uparrow\uparrow}\rangle$ and $\frac{1}{\sqrt{6}}(|{\downarrow\uparrow\uparrow}\rangle - 2\,|{\uparrow\downarrow\uparrow}\rangle + |{\uparrow\uparrow\downarrow}\rangle)$ are degenerate in energy. This degeneracy is then lifted by the couplings J_2, J_3. The effective Hamiltonian to first order is an XXZ chain in a magnetic field [30–35,29]. We obtain the following effective couplings for the XXZ chain:

$$\begin{aligned} J_{xy} &= \frac{1}{6}J_2 - \frac{2}{3}J_3 \\ J_z &= \frac{1}{36}(J_2 + 8J_3) \\ h_{\text{eff}} &= h - h_c - \frac{1}{36}(5J_2 + 22J_3) \end{aligned} \tag{6.1}$$

and therefore the effective anisotropy $\Delta_{\text{eff}} = J_z/|J_{xy}|$ is

$$\Delta_{\text{eff}} = \frac{J_2 + 8J_3}{|6J_2 - 24J_3|}\,. \tag{6.2}$$

For $5/32 < J_3/J_2 < 7/16$, we have $\Delta_{\text{eff}} > 1$ and thus a gap, *i.e.* an $\langle M \rangle = 2/3$ plateau in the original model. A plateau with $\langle M \rangle = 2/3$ can be indeed observed numerically somewhere in this region (see e.g. [20]). The line $J_3/J_2 = 1/4$ describes the Ising limit $\Delta_{\text{eff}} = \infty$.

In order to address the region of ferromagnetic J_1, we now start from the limit $J_1 = J_3 = 0$ and apply a magnetic field $h_c = J_2$. Then the two states $|{\uparrow\uparrow}\rangle$ and $\frac{1}{\sqrt{2}}(|{\downarrow\uparrow}\rangle - |{\uparrow\downarrow}\rangle)$ on the J_2-dimer become degenerate in energy while the intermediate spins are already polarized. This can be again treated by degenerate perturbation theory in $1/J_2$. Up to third order we find an XXZ chain with

$$\begin{aligned} \frac{J_{xy}}{J_2} &= \frac{1}{8}\left(2 + \bar{J}_1 + \bar{J}_3\right)\left(\bar{J}_1 - \bar{J}_3\right)^2 \\ \frac{J_z}{J_2} &= \frac{1}{8}\left(\bar{J}_1 + \bar{J}_3\right)\left(\bar{J}_1 - \bar{J}_3\right)^2 \\ \frac{h_{\text{eff}}}{J_2} &= \frac{h}{J_2} - 1 - \frac{1}{2}\left(\bar{J}_1 + \bar{J}_3\right) - \frac{1}{4}\left(\bar{J}_1 - \bar{J}_3\right)^2 \end{aligned} \tag{6.3}$$

that is

$$\Delta_{\text{eff}} = \frac{\bar{J}_1 + \bar{J}_3}{|2 + \bar{J}_1 + \bar{J}_3|}\,. \tag{6.4}$$

In the region where this treatment is valid, we always have a small Δ_{eff}, *i.e.* no plateau at $\langle M \rangle = 2/3$. Indeed,

one can see that the dimer excitations can hop at second order in $1/J_2$ while up to this order all diagonal terms involve only a single dimer site. Thus, up to second order the diagonal terms contribute only to $h_{\rm eff}$ and to this order one obtains an XY chain in a magnetic field. A small anisotropy is restored at third order before terms that are not described by a simple XXZ chain arise at fourth order.

VII. CONCLUSIONS

We have studied the frustrated trimer chain (1.1) (Fig. 1) using a variety of methods. First, we have computed 12th-order high-temperature series for the susceptibility χ and specific heat. Fits of the high-temperate tail of the susceptibility computed from the model to the one measured on $Cu_3Cl_6(H_2O)_2{\cdot}2H_8C_4SO_2$ [15] lead to $J_2 = 250\text{K} \pm 40\text{K}$ and *ferromagnetic* $J_1 = -260\text{K} \pm 50\text{K}$, $J_3 = -40\text{K} \pm 30\text{K}$ (we showed in appendix A that $\chi(T)$ cannot be fitted with the antiferromagnetic parameters proposed in [18–20]). We assumed that these parameters remain valid down to low temperatures since we are not aware of any indication of a drastic change in the magnetic behavior of $Cu_3Cl_6(H_2O)_2{\cdot}2H_8C_4SO_2$ as temperature is lowered. In fact, features of other experimental observations at intermediate and low temperatures are roughly reproduced with the aforementioned parameters: We find a maximum in $\chi(T)$ in the region $50\text{K} \leq T \leq 100\text{K}$ and a smooth increase of the low-temperature magnetization $\langle M \rangle$ from 0 to 1/3 as the external magnetic field is increased from zero to several ten Tesla. From a quantitative point of view, the agreement may however not yet be entirely satisfactory: Deviations between the measured susceptibility from the one obtained within the model can be seen in the interval $80\text{K} \leq T \leq 200\text{K}$ and the model predicts an $\langle M \rangle = 1/3$ magnetization for a magnetic field that is a factor two to three below the one actually required in the experiment.

Probably the most exciting experimental observation [15] for $Cu_3Cl_6(H_2O)_2{\cdot}2H_8C_4SO_2$ is the existence of a spin gap of about 5.5K. We have therefore searched for a spin gap in the region of ferromagnetic J_1 and J_3 using several methods. Neither Lanczos diagonalization, discussion of the line $J_1 = J_3$ nor an effective Hamiltonian for large J_2 provide any evidence in favor of a spin gap in this parameter region. A further careful analysis of this issue would certainly be desireable in particular in view of the small size of the actually observed gap. At present, however, it seems likely that the model does not reproduce a spin gap in the relevant parameter region.

It should be noted that the coupling constants which we have determined are about two orders of magnitude larger than the experimentally observed gap. Therefore, a small modification of the model is sufficient to produce a gap of this magnitude. The possibilities include dimerization of the coupling constants, exchange anisotropy as well as additional couplings. A modification of the model along these lines may also help to improve the quantitative agreement with the features observed in $Cu_3Cl_6(H_2O)_2{\cdot}2H_8C_4SO_2$ at energy scales of about 100K. Further measurements are however needed to discriminate between these possibilities. For example, it would be interesting to measure the specific heat and compare it with our series (2.3). It emerges also from our analysis that a temperature of 300K is still too small to allow for application of a simple Curie-Weiss law to the magnetic susceptibility χ. It would therefore be useful to measure χ to higher temperatures in order to permit analysis via truncation of (2.2) after the order T^{-2} which would provide a more direct check that $2(J_1 + J_3) + J_2$ is negative.

However, inelastic neutron scattering would presumably be most helpful: First, this should clearly decide if $Cu_3Cl_6(H_2O)_2{\cdot}2H_8C_4SO_2$ is really quasi-one-dimensional and secondly it would yield direct information on the excitation spectrum which could hopefully be interpreted in terms of coupling constants. Such a determination of the coupling constants would also circumvent the question whether model parameters change as a function of temperature since neutron scattering is carried out at low temperatures, *i.e.* the temperature scale of interest. We therefore hope that neutron scattering can indeed be performed and are curious if excitations will be observed that are similar to those computed in the trimer chain model (Fig. 4).

The frustrated trimer chain model is also interesting in its own right: It has a rich phase diagram which among others includes many aspects of the J_1-J_2 chain such as a frustration-induced spin gap in some parameter region [18–20]. Also plateaux in the magnetization curve exist in this model: A plateau with $\langle M \rangle = 1/3$ is abundant both in the regions with antiferromagnetic and ferrimagnetic $h = 0$ groundstates. Also a plateau with $\langle M \rangle = 2/3$ can be shown to exist in the region with $J_1, J_3 > 0$ (see [20] and section VI). Like in the case of the spin gap, the opening of the latter plateau is accompanied by spontaneous breaking of translational invariance in the groundstate. Amusingly, however, the $\langle M \rangle = 2/3$ plateau opens already for $J_2, J_3 \ll J_1$ – a region where the spin gap is absent. In this context of magnetization plateaux, we hope that the magnetization measurements [15] can be extended to slightly higher fields which should unveil the lower edge of the $\langle M \rangle = 1/3$ plateau.

ACKNOWLEDGMENTS

We are very grateful to M. Ishii and H. Tanaka for providing us with their partially unpublished data for the susceptibility and for discussions. In addition, useful discussions with D.C. Cabra, F. Mila, M. Troyer and T.M. Rice are gratefully acknowledged. A.H. is indebted to the Alexander von Humboldt-foundation for financial

support during the initial stages of this work as well as to the ITP-ETHZ for hospitality.

APPENDIX A: ANTIFERROMAGNETIC COUPLING CONSTANTS

In this appendix we discuss a fit of the magnetic susceptibility χ with antiferromagnetic coupling constants $J_i > 0$. A number of assumptions are necessary in order to obtain at all a convergent fit with parameters in the antiferromagentic spin gap region [18–20].

First we fix the ratio of the magnetic field $h(\langle M\rangle = 1/3)$ to the spin gap $h_c(\langle M\rangle = 0)$ approximately to the experimental value [15]

$$\frac{h(\langle M\rangle = 1/3)}{h_c(\langle M\rangle = 0)} = 14.1\,. \tag{A1}$$

To this end, we used numerical data for $h(\langle M\rangle = 1/3)$ and $h_c(\langle M\rangle = 0)$ on systems of size $L = 12$, 18 and 24. This data was extrapolated to $L = \infty$ in the same manner as in [19], *i.e.* with a polynomial fit $h_L(\langle M\rangle) = h_\infty(\langle M\rangle) + a/L + b/L^2$. For the spin gap, this amounts to reproducing the computation of [19]. The numerical solutions to eq. (A1) were then approximated by

$$\tilde{J}_3 = 0.3\left(\tilde{J}_2 - 0.85\right)^2 + 0.63 \tag{A2}$$

where we used the notation (5.1). An analytic formula was needed in order to implement the constraint (A1) by inserting (A2) into (2.2) before performing a fit. Eq. (A2) is valid for $0.6 \lesssim \tilde{J}_2 \lesssim 2$.

The constraint (A2) is still not sufficient to ensure antiferromagnetic $J_i > 0$ with $0.6 \le \tilde{J}_2 \le 2$. To achieve this goal, we had to make the following further adjustments when fitting our series (2.2) to the experimental data [15]:

1. Keep g as a fitting parameter,
2. add a constant to (2.2) and use this as another parameter in the fit,
3. start fitting at low temperatures $T_l \approx 100$K.

Note that both g and the additive constant turn out to be quite large. For example, for the parameters used in Fig. 5, we found $g \approx 2.9$ and an additive constant of about $-0.17 \cdot 10^{-3}\mathrm{K}^{-1}/k_B$. This means that the prefactor in (2.4) is off by a factor of about 2 from the value determined by ESR and that the absolute value of the additive constant is almost 40% of the susceptibility observed at $T = 300$K !

On the basis of these unrealistic parameters, one could already discard this fit to $\chi(T)$. Nevertheless, we compare it to the one shown in Fig. 2: Fig. 5 shows the measured susceptibility for the polycrystalline sample [15] together with the series evaluated at $J_1 = 120$K, $J_2 = 141$K and $J_3 = 79$K. This parameter set is close to parameters proposed in [19]. This proposal was based on two assumptions: 1) The model should give rise to the experimentally observed spin gap of around 5K [15]. 2) The maximum of χ is located at $T \approx 0.7J_1$. While we do indeed reproduce the spin gap rather accurately, the second assumption is falsified by our computation: The frustration pushes the maximum of $\chi(T)$ again to lower temperatures as compared to a non-frustrated system.

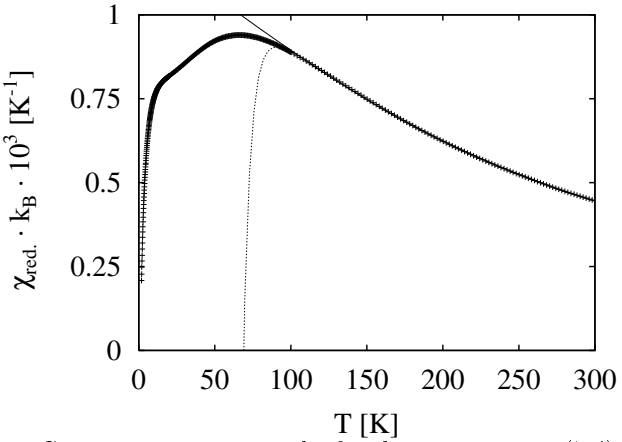

FIG. 5. Experimental results for the susceptibility ('+') in comparison with the fit $J_1 = 120$K, $J_2 = 141$K and $J_3 = 79$K. We show the raw 12th order series (dotted line) as well as the [7,6] Padé approximant (full line).

Fig. 5 should be compared to Fig. 2. The seemingly better agreement in the region $100\mathrm{K} \le T \le 200\mathrm{K}$ is due to including this temperature interval in the fit for Fig. 5, but not in Fig. 2. Note that the $|J_i|$ are now smaller by a factor of about two than those used in Fig. 2. One would therefore expect better convergence in the vicinity of the maximum of $\chi(T)$, *i.e.* for $50\mathrm{K} \le T \le 100\mathrm{K}$. This expectation is confirmed by the fact that in Fig. 5, the [7,6], [6,6] and [6,5] Padé approximants are indistinguishable. However, while the series reproduces the maximum roughly in Fig. 2, this is definitely not the case in Fig. 5. The better agreement of the fit in Fig. 2 with the experimental data at $T \approx 70$K is particularly remarkable since this temperature range is far from the fitting region in this case, while closeby temperatures were used in Fig. 5. In combination with the unrealistic assumptions needed to obtain a convergent fit with all $J_i > 0$ one can therefore conclude safely that only antiferromagnet coupling constants are not suitable for describing the experimental data [15] for the susceptibility $\chi(T)$.

APPENDIX B: EFFECTIVE HAMILTONIAN FOR J_1 LARGE AND FERROMAGNETIC

For a strong ferromagnetic intra-trimer interaction J_1, the noninteracting groundstates are built from products of trimer $S = 3/2$ states. Up to second order we find the following effective Hamiltonian in this subspace of low-lying trimer quartets:

$$
\begin{aligned}
H_{\text{eff.}} = & \mathcal{J}_a \sum_i \mathbf{S}_i \cdot \mathbf{S}_{i+1} + \mathcal{J}_b \sum_i \mathbf{S}_i \cdot \mathbf{S}_{i+2} \\
& + \mathcal{J}_c \sum_i \left(\mathbf{S}_i \cdot \mathbf{S}_{i+1}\right)^2 \\
& + \frac{\mathcal{J}_d}{2} \sum_i \big\{ (\mathbf{S}_i \cdot \mathbf{S}_{i+1})(\mathbf{S}_{i+1} \cdot \mathbf{S}_{i+2}) \\
& \quad + (\mathbf{S}_{i+2} \cdot \mathbf{S}_{i+1})(\mathbf{S}_{i+1} \cdot \mathbf{S}_i) \big\} , \qquad \text{(B1)}
\end{aligned}
$$

where the $\mathbf{S}_i$ are now effective spin-3/2 operators.

The coupling constants are found to be:

$$
\begin{aligned}
\mathcal{J}_a &= \frac{1}{9}(J_2 + 2J_3) + \frac{197J_2^2 + 212J_2J_3 + 212J_3^2}{2592|J_1|} , \\
\mathcal{J}_b &= \frac{2J_2^2 + 5J_2J_3 + 2J_3^2}{27|J_1|} , \\
\mathcal{J}_c &= \frac{41J_2^2 + 100J_2J_3 + 36J_3^2}{1296|J_1|} , \\
\mathcal{J}_d &= -\frac{4(2J_2^2 + 5J_2J_3 + 2J_3^2)}{243|J_1|} . \qquad \text{(B2)}
\end{aligned}
$$

Even if this effective Hamiltonian is not a well-known one, it is clear that there is no spin gap in first order, since then the system is effectively a nearest neighbor $S = 3/2$ Heisenberg chain which is either gapless ($J_2 + 2J_3 > 0$) or ferromagnetic ($J_2 + 2J_3 < 0$).

If one neglects the $\mathcal{J}_c$ and $\mathcal{J}_d$ terms, one obtains a frustrated $S = 3/2$ chain which has been investigated with DMRG and leads to a gap for $\mathcal{J}_b/\mathcal{J}_a \gtrsim 0.3$ [36]. It seems to be possible to obtain antiferromagnetic $\mathcal{J}_a$ and $\mathcal{J}_b$ in this region if J_2 and J_3 are chosen suitably and large (a region including the coupling constants determined in section II B). However, then one is not in the perturbative region anymore and the $\mathcal{J}_c$ and $\mathcal{J}_d$ terms may also become important. Further discussion is therefore needed for reliable conclusions about a gap on the basis of the Hamiltonian (B1) with coupling constants (B2).

[1] K. Hida, J. Phys. Soc. Jpn. **63**, 2359 (1994).
[2] K. Okamoto, Solid State Communications **98**, 245 (1996).
[3] D.C. Cabra and M.D. Grynberg, Phys. Rev. **B59**, 119 (1999).
[4] A. Honecker, Phys. Rev. **B59**, 6790 (1999).
[5] K. Okamoto and A. Kitazawa, J. Phys. A: Math. Gen. **32**, 4601 (1999).
[6] B. Sutherland and B.S. Shastry, J. Stat. Phys. **33**, 477 (1983).
[7] M.W. Long and R. Fehrenbacher, J. Phys.: Condensed Matter **2**, 2787 (1990).
[8] M.W. Long and S. Siak, J. Phys.: Condensed Matter **2**, 10321 (1990).
[9] K. Takano, J. Phys. A: Math. Gen. **27**, L269 (1994).
[10] K. Takano, K. Kubo and H. Sakamoto, J. Phys.: Condensed Matter **8**, 6405 (1996).
[11] M.R. Bond, R.D. Willett, R.S. Rubins, P. Zhou, C.E. Zaspel, S.L. Hutton and J.E. Drumheller, Phys. Rev. **B42**, 10280 (1990).
[12] Y. Ajiro, T. Asano, T. Inami, H. Aruga-Katori and T. Goto, J. Phys. Soc. Jpn. **63**, 859 (1994).
[13] D.D. Swank and R.D. Willett, Inorganica Chimica Acta **8**, 143 (1974).
[14] D.D. Swank, C.P. Landee and R.D. Willett, Journal of Magnetism and Magnetic Materials **15**, 319 (1980).
[15] M. Ishii, H. Tanaka, M. Hori, H. Uekusa, Y. Ohashi, K. Tatani, Y. Narumi and K. Kindo, J. Phys. Soc. Jpn. **69**, 340 (2000).
[16] The low-temperature susceptibility of [15] is substantially lower than that of [14]. The authors of [15] suggested that this discrepancy may be due to a large impurity contribution in [14].
[17] We use the notations of [18] which differ from [15] by exchanging J_2 and J_3.
[18] K. Okamoto, T. Tonegawa, Y. Takahashi and M. Kaburagi, J. Phys.: Condensed Matter **11**, 10485 (1999).
[19] K. Sano and K. Takano, J. Phys. Soc. Jpn. **69**, 2710 (2000).
[20] T. Tonegawa, K. Okamoto, T. Hikihara, Y. Takahashi and M. Kaburagi, J. Phys. Soc. Jpn. **69** Suppl. A, 332 (2000).
[21] `http://www.tu-bs.de/~honecker/3mer/`
`http://www.itp.phys.ethz.ch/staff/laeuchli/3mer`
[22] The price to pay for using an elementary approach is a substantial amount of CPU time even on modern workstations.
[23] G.A. Baker Jr., G.S. Rushbrooke and H.E. Gilbert, Physical Review **135**, A1272 (1964); A. Bühler, N. Elstner and G.S. Uhrig, Eur. Phys. J. **B16**, 475 (2000).
[24] M. Ishii and H. Tanaka, private communication.
[25] A. Honecker, F. Mila and M. Troyer, Eur. Phys. J. **B15**, 227 (2000).
[26] $\mathcal{J}_2$ changes sign inside the region with $\mathcal{J}_1 > 0$ such that $\mathcal{J}_2 < 0$ throughout the region with $\mathcal{J}_1 < 0$. $\mathcal{J}_2$ is therefore not relevant to the transition.
[27] S. Eggert, Phys. Rev. **B54**, R9612 (1996).
[28] We stopped at fifth order because terms that are not contained in (5.2) would start to appear at the sixth order.
[29] D.C. Cabra, A. Honecker and P. Pujol, Eur. Phys. J. **B13**, 55 (2000).
[30] K. Totsuka, Phys. Rev. **B57**, 3454 (1998); Eur. Phys. J. **B5**, 705 (1998).
[31] F. Mila, Eur. Phys. J. **B6**, 201 (1998).
[32] G. Chaboussant, M.-H. Julien, Y. Fagot-Revurat, M. Hanson, L.P. Lévy, C. Berthier, M. Horvatić and O. Piovesana, Eur. Phys. J. **B6**, 167 (1998).
[33] K. Tandon, S. Lal, S.K. Pati, S. Ramasesha and D. Sen, Phys. Rev. **B59**, 396 (1999).
[34] A. Furusaki and S.C. Zhang, Phys. Rev. **B60**, 1175 (1999).
[35] S. Wessel and S. Haas, Eur. Phys. J. **B16**, 393 (2000); Phys. Rev. **B62**, 316 (2000).
[36] R. Roth and U. Schollwöck, Phys. Rev. **B58**, 9264 (1998).